PID LPV observer for a semi-active suspension system

Thanh-Phong Pham, Olivier Sename, Thanh-Ha Duong-Thi

PID LPV observer for a semi-active suspension system ⋆

Thanh-Phong Pham * **Olivier Sename** **
Thanh-Ha Duong-Thi ***

* *Faculty of Electrical and Electronic Engineering, The University of Danang - University of Technology and Education, 550000 Danang, Vietnam (e-mail: ptphong@ute.udn.vn).*
** *Univ. Grenoble Alpes, CNRS, Grenoble INP⊤, GIPSA-Lab, 38000 Grenoble, France ⊤Institute of Engineering Univ. Grenoble Alpes (e-mail: olivier.sename@grenoble-inp.fr).*
*** *Faculty of Electrical and Electronic Engineering, The University of Danang - University of Technology and Education, 550000 Danang, Vietnam (e-mail: thanhha.dthi@gmail.com).*

Abstract: This paper presents a proportional integral derivative observer for linear parameter-varying systems, applied to estimate the damper force in a semi-active suspension system. The stability of the observer is proved using a parameter-dependent Lyapunov function,a and its performance is ensured through minimization of the induced $\mathcal{L}_2$ gain from unknown disturbances towards the estimation error. The effectiveness of this approach is demonstrated through frequency domain analysis and validated via realistic simulations.

Keywords: PID observer; linear parameter-varying system; automotive suspension systems

1. INTRODUCTION

The linear parameter-varying (LPV) framework has emerged as a powerful tool to handle nonlinearities, time-varying parameters and adaptive-like objectives (see (Sename, 2025; Sename et al., 2013; Mohammadpour and Scherer, 2012), and references therein). In view of state estimation and fault detection, unknown input observers have been developed (Marx et al., 2019; Ichalal and Mammar, 2015; de Oliveira and Pereira, 2021; Kulcsár et al., 2010). Observers are generally classified as proportional observers (PO), proportional integral observers (PIO), and dynamic observers (DO). More recently, the unified observer proposed by Gao et al. (2016), which offers a general structure and additional flexibility, has been extended to LPV systems, demonstrating applications such as wind turbines (Pérez-Estrada et al., 2018) and semi-active suspensions (Pham et al., 2019). However, the design process for unified observers is complex and involves higher computational costs, leading to the idea of developing new observer structures, such as proportional integral derivative observers (PIDO).

On the other hand, the design of observers for semi-active suspension systems is essential to improve both control performance and fault detection capabilities (Savaresi et al., 2010; Tseng and Hrovat, 2015). Consequently, numerous observers have been proposed in the literature to tackle the unique challenges associated with semi-active suspension systems, including nonlinearity, unknown input road profile disturbances, and measurement noise (Yi and Suk Song, 1999; Dugard et al., 2012; Tudón-Martínez et al., 2015; Pham et al., 2019; Savaresi et al., 2019; Pham et al., 2021; Csekő et al., 2015; Koch et al., 2010). Many of these methodologies address the aforementioned challenges efficiently, thanks to the use of LPV observers.

This study aims at proposing a PID LPV observer where the matrices are structured to incorporate proportional, integral, and derivative actions. This novel observer is then applied to estimate the damper force of an electro-rheological semi-active damper in an automotive suspension system. The main contributions of this paper are as follows:

- For the first time, a PID observer for LPV systems has been developed to minimize the effects of sensor noise and unknown disturbances through an induced $\mathcal{L}_2$ gain objective.
- The design method makes use of the Finsler's Lemma to reformulate a quadratic equality from the observer matrix structure and a quadratic inequality from the stability condition into a linear matrix inequality (LMI) optimization problem, ensuring computational feasibility. The stability proof uses a parameter-dependent Lyapunov function.
- The proposed observer has been simulated on a realistic scaled vehicle model to demonstrate its performance in various simulation scenarios.

The rest of this paper is organized as follows. Section 4 presents an ER automotive suspension system. Section 2 details the definition of the PID observer. Section 3 introduces the design of the PID observer. Section 4.5,

⋆ This research is funded by The University of Danang – University of Technology and Education under project number T2024-06-05.

simulation results are presented. Finally, Section 5 provides some concluding remarks.

2. PROBLEM STATEMENT

Let us consider an LPV system given as:

$$\begin{cases} \dot{x} &= A(\rho)x + B(\rho)u + D_1\omega \\ y &= Cx + D_2\omega \end{cases} \tag{1}$$

where $x \in \mathcal{R}^{n_x}$ is the system state vector, $u \in \mathcal{R}^{n_u}$ the control input, $\omega \in \mathcal{R}^{n_\omega}$ the unknown disturbance input, and $y \in \mathcal{R}^{n_y}$ the measurment vector.

In the same spirit as (Gao et al., 2016; Pérez-Estrada et al., 2018) the observer is chosen as follows:

$$\begin{cases} \dot{\hat{x}} = A(\rho)\hat{x} + B(\rho)u + \nu \\ \dot{\epsilon} = A_L\epsilon + B_L(\rho)(y - \hat{y}) \\ \nu = C_L\epsilon + D_L(\rho)(y - \hat{y}) \\ \hat{y} = C\hat{x} \end{cases} \tag{2}$$

where $\hat{x} \in \mathcal{R}^{n_x}$ is estimated states of x, while $\epsilon \in \mathcal{R}^{2n_x}$ represents the auxiliary observer state. $\nu \in \mathcal{R}^{n_x}$ serves as an correction signal to enhance the observer's performance. To cope with a PID observer form, the observer matrices $A_L \in \mathcal{R}^{2n_x \times 2n_x}$, $B_L(\rho) \in \mathcal{R}^{2n_x \times n_y}$, $C_L \in \mathcal{R}^{n_x \times 2n_x}$, $D_L(\rho) \in \mathcal{R}^{n_x \times n_y}$ are defined with a specific structure as follows:

$$A_L = \begin{bmatrix} 0_{n_x \times n_x} & 0_{n_x \times n_x} \\ 0_{n_x \times n_x} & -\tau I_{n_x} \end{bmatrix} \in \mathcal{R}^{2n_x \times 2n_x} \tag{3}$$

where τ is chosen a priori and,

$$B_L(\rho) = \begin{bmatrix} R_I(\rho) \\ R_D(\rho) \end{bmatrix} \tag{4}$$

where $R_I(\rho) \in \mathcal{R}^{n_x \times n_y}$, $R_D(\rho) \in \mathcal{R}^{n_x \times n_y}$, and

$$C_L = [I_{n_x} \; I_{n_x}], \tag{5}$$

$$D_L(\rho) = [R_P(\rho)] \in \mathcal{R}^{n_x \times n_y} \tag{6}$$

The structural concept is based on the ideas presented in Apkarian and Noll (2006). By incorporating the PID structure (2) within the H_∞ framework, we derive an PID/H_∞ observer. This observer shall minimize the impact of unknown input disturbances on the estimation error by utilizing the H_∞-norm.

Now, the estimation error e is defined as follows:

$$e = x - \hat{x} \tag{7}$$

From (1) and (2), one obtains:

$$\dot{e} = (A(\rho) - D_L(\rho)C)e - C_L\epsilon + (D_1 - D_L(\rho)D_2)\,\omega \tag{8}$$

From (8) and the second equation $\dot{\hat{\epsilon}}$ in (2), the dynamical equations to be considered are:

$$\begin{cases} \dot{e} = & (A(\rho) - D_L(\rho)C)e - C_L\epsilon + (D_1 - D_L(\rho)D_2)\omega \\ \dot{\epsilon} = & B_L(\rho)Ce + A_L\epsilon + B_L(\rho)D_2\omega \end{cases} \tag{9}$$

Denoting $\xi = \begin{pmatrix} e \\ \epsilon \end{pmatrix}$, the estimation error dynamical system (9) becomes

$$\dot{\xi} = \mathbb{A}(\rho)\xi + \mathbb{D}(\rho)\omega \tag{10}$$

$$\mathbb{A}(\rho) = \begin{bmatrix} A(\rho) - D_L(\rho)C & -C_L \\ B_L(\rho)C & A_L \end{bmatrix}, \mathbb{D}(\rho) = \begin{bmatrix} D_1 - D_L(\rho)D_2 \\ B_L(\rho)D_2 \end{bmatrix}.$$

Problem definition: The PID/$\mathcal{H}_\infty$ observer design problem is to find the observer matrices A_L, $B_L(\rho)$, C_L, $D_L(\rho)$ such that:

- The estimation error dynamical system (10) is asymptotically stable for $\omega(t) = 0$;
- The input-output gain from the unknown input disturbance to the estimation error, is such that
  $$\|e(t)\|_2 < \gamma\|\omega(t)\|_2, \forall\omega(t) \neq 0,$$
  where the $\mathcal{L}_2$-induced performance level γ is to be minimized.

3. MAIN RESULT

This problem is solved following an LMI framework via the following theorem.

Theorem 1. Consider the system model (1) and the observer (2). The observer design problem is solved if there exist symmetric positive definite matrices $P_1(\rho)$, $P_2(\rho)$, matrices $Y_1(\rho)$, $Y_2(\rho)$, a symmetric matrix Z, and positive scalars ϵ_l and γ, solutions of the following LMI optimization problem:

$$\begin{aligned} &\min_{P_1(\rho),P_2(\rho),Y_1(\rho),Y_2(\rho),Z,\epsilon_l} \gamma \\ &\text{s. t. } M(\rho) + B_n^T Z B_n < 0 \end{aligned} \tag{11}$$

where $B_n = \begin{bmatrix} 0_{2n_x \times n_x} & I_{2n_x} & 0_{2n_x \times n_y} \end{bmatrix}$, and

$M(\rho) = \begin{bmatrix} M_{11}(\rho) & M_{12}(\rho) & M_{13}(\rho) \\ M_{12}(\rho)^T & M_{22}(\rho) & M_{23}(\rho) \\ M_{13}(\rho)^T & M_{23}(\rho)^T & -\gamma^2 I \end{bmatrix}$, with

$M_{11}(\rho) = A(\rho)^T P_1(\rho) + P_1(\rho)A(\rho) + Y_1(\rho)C + C^T Y_1(\rho)^T + \dot{\rho}\frac{\partial P_1}{\partial \rho} + I$,

$M_{12}(\rho) = C^T Y_2(\rho)^T - P_1(\rho)C_L$,

$M_{13}(\rho) = P_1(\rho)D_1 + Y_1(\rho)D_2$,

$M_{22}(\rho) = A_L^T P_2(\rho) + P_2(\rho)A_L + \dot{\rho}\frac{\partial P_2}{\partial \rho}$,

$M_{23}(\rho) = Y_2(\rho)D_2$.

Then the observer matrices are $B_L(\rho) = P_2(\rho)^{-1}Y_2(\rho)$ and $D_L(\rho) = -P_1(\rho)^{-1}Y_1(\rho)$.

Proof: Consider the Lyapunov function candidate as the following:

$$V = \xi^T \begin{bmatrix} P_1(\rho) & 0 \\ 0 & P_2(\rho) \end{bmatrix} \xi \tag{12}$$

Taking the derivative of (12), one obtains

$$\begin{aligned} \dot{V} = \dot{\xi}^T &\begin{bmatrix} P_1(\rho) & 0 \\ 0 & P_2(\rho) \end{bmatrix} \xi + \xi^T \begin{bmatrix} P_1(\rho) & 0 \\ 0 & P_2(\rho) \end{bmatrix} \dot{\xi} \\ &+ \xi^T \begin{bmatrix} \dot{\rho}\frac{\partial P_1}{\partial \rho} & 0 \\ 0 & \dot{\rho}\frac{\partial P_2}{\partial \rho} \end{bmatrix} \xi \end{aligned} \tag{13}$$

Substituting (10) into (13), one obtains

$$\begin{aligned} \dot{V} = {} & \xi^T \mathbb{A}(\rho)^T \begin{bmatrix} P_1(\rho) & 0 \\ 0 & P_2(\rho) \end{bmatrix} \xi + \omega^T \mathbb{D}(\rho)^T \begin{bmatrix} P_1(\rho) & 0 \\ 0 & P_2(\rho) \end{bmatrix} \xi \\ &+ \xi^T \begin{bmatrix} P_1(\rho) & 0 \\ 0 & P_2(\rho) \end{bmatrix} \mathbb{A}(\rho)\xi + \xi^T \begin{bmatrix} P_1(\rho) & 0 \\ 0 & P_2(\rho) \end{bmatrix} \mathbb{D}(\rho)\omega \\ &+ \xi^T \begin{bmatrix} \dot{\rho}\frac{\partial P_1}{\partial \rho} & 0 \\ 0 & \dot{\rho}\frac{\partial P_2}{\partial \rho} \end{bmatrix} \xi \end{aligned} \tag{14}$$

Denoting $\eta = \begin{bmatrix} \xi \\ \omega \end{bmatrix}$, (14) becomes

$$\dot{V} = \eta^T \begin{bmatrix} \Psi_{11}(\rho) & \Psi_{12}(\rho) & \Psi_{13}(\rho) \\ \Psi_{12}(\rho)^T & \Psi_{22}(\rho) & \Psi_{23}(\rho) \\ \Psi_{13}(\rho)^T & \Psi_{23}(\rho)^T & 0 \end{bmatrix} \eta \qquad (15)$$

where $\Psi_{11}(\rho) = A(\rho)^T P_1(\rho) - C^T D_L(\rho)^T P_1(\rho) + P_1(\rho)A(\rho) - P_1(\rho)D_L(\rho)C + \dot{\rho}\frac{\partial P_1}{\partial \rho}$; $\Psi_{12}(\rho) = C^T B_L(\rho)^T P_2(\rho) - P_1(\rho)C_L$; $\Psi_{13}(\rho) = P_1(\rho)D_1 - P_1(\rho)D_L(\rho)D_2$; $\Psi_{22}(\rho) = A_L^T P_2(\rho) + P_2(\rho)A_L + \dot{\rho}\frac{\partial P_2}{\partial \rho}$; $\Psi_{23}(\rho) = P_2(\rho)B_L(\rho)D_2$.
The second objective w.r.t to H_∞ performance is solved if

$$\begin{aligned} &\dot{V} + e^T e - \gamma^2 \omega^T \omega < 0 \\ \Leftrightarrow &\dot{V} + \xi^T \begin{bmatrix} I & 0 \\ 0 & 0 \end{bmatrix} \xi - \gamma^2 \omega^T \omega < 0 \\ \Leftrightarrow &\eta^T \begin{bmatrix} \Psi_{11}(\rho) + I & \Psi_{12}(\rho) & \Psi_{13}(\rho) \\ \Psi_{12}(\rho)^T & \Psi_{22}(\rho) & \Psi_{23}(\rho) \\ \Psi_{13}(\rho)^T & \Psi_{23}(\rho)^T & -\gamma^2 I \end{bmatrix} \eta < 0 \end{aligned} \qquad (16)$$

Besides, due to the PID observer structure (2), where A_L has only zero elements in the first n_x rows (see (3)), the following equation holds:

$$[I_{n_x} \ 0_{n_x \times n_x}] A_L \epsilon = 0 \Leftrightarrow K\epsilon = 0 \qquad (17)$$

where $K = [0_{n_x \times n_x} \ 0_{n_x \times n_x}]$.
Equation (17) can be rewritten as:

$$K B_n \eta = 0 \qquad (18)$$

where $B_n = \begin{bmatrix} 0_{2n_x \times n_x} & I_{2n_x} & 0_{2n_x \times n_y} \end{bmatrix}$.
Using Finsler's Lemma (Iwasaki and Shibata, 2002), both conditions (16) and (18) are equivalent to the existence of a symmetric matrix $Z \in \mathbb{R}^{2n_x \times 2n_x}$ such that

$$\begin{cases} Q(\rho) + B_n^T Z B_n < 0 \\ K_\perp^T Z K_\perp \geq 0 \end{cases} \qquad (19)$$

where $Q(\rho) = \begin{bmatrix} \Psi_{11}(\rho) + I & \Psi_{12}(\rho) & \Psi_{13}(\rho) \\ \Psi_{12}(\rho)^T & \Psi_{22}(\rho) & \Psi_{23}(\rho) \\ \Psi_{13}(\rho)^T & \Psi_{23}(\rho)^T & -\gamma^2 I \end{bmatrix}$.
Since $K = [0_{n_x \times n_x} \ 0_{n_x \times n_x}]$, then $K_\perp = \begin{bmatrix} 0_{n_x \times n_x} \\ 0_{n_x \times n_x} \end{bmatrix}$.
Therefore, the second inequality in (19) is satisfied.
Denoting $Y_1(\rho) = -P_1(\rho)D_L(\rho)$ and $Y_2(\rho) = P_2(\rho)B_L(\rho)$ and substituting into above inequality (19), one obtains

$$M(\rho) + B_n^T Z B_n < 0 \qquad (20)$$

where $M(\rho, \dot{\rho}) = \begin{bmatrix} M_{11}(\rho) & M_{12}(\rho) & M_{13}(\rho) \\ M_{12}(\rho)^T & M_{22}(\rho) & M_{23}(\rho) \\ M_{13}(\rho)^T & M_{23}(\rho)^T & -\gamma^2 I \end{bmatrix}$, with $M_{11}(\rho) = A(\rho)^T P_1(\rho) + P_1(\rho)A(\rho) + Y_1(\rho)C + C^T Y_1(\rho)^T + \dot{\rho}\frac{\partial P_1}{\partial \rho} + I$; $M_{12}(\rho) = C^T Y_2(\rho)^T - P_1(\rho)C_L$; $M_{13}(\rho) = P_1(\rho)D_1 + Y_1(\rho)D_2$; $M_{22}(\rho) = A_L^T P_2(\rho) + P_2(\rho)A_L + \dot{\rho}\frac{\partial P_2}{\partial \rho}$; $M_{23}(\rho) = Y_2(\rho)D_2$.
If (11) is satisfied, from (18) and (19) implies that

$$\dot{V} + e^T e - \gamma^2 \omega^T \omega < 0. \qquad (21)$$

Following the same steps as in Darouach et al. (2011), we obtain

$$\|e(t)\|_{\mathcal{L}_2}^2 < \gamma^2 \|\omega(t)\|_{\mathcal{L}_2}^2. \qquad (22)$$

The proof of Theorem 1 is completed. ■
Note that, since the LMI problem (11) to be solved depends on ρ and $\dot{\rho}$, a classical method consists in using a grid-based approach for ρ together with the min/max values for the parameter derivative, i.e $|\dot{\rho}| \leq \nu$ (Wu, 1995). The observer design steps can be summarized in the following algorithm.

Design procedure:
Input: The system matrices $A(\rho)$, $B(\rho)$, D_1, C, D_2, the range and a grid of values of ρ.
Output: The observer matrices A_L, $B_L(\rho)$, C_L, $D_L(\rho)$.
Step 1: Choose τ, then determine the observer matrices A_L and C_L according to (3) and (5), respectively.
Step 2: Solve the LMIs (11) to obtain the solutions $P_1(\rho)$, $P_2(\rho)$, $Y_1(\rho)$, $Y_2(\rho)$, Z and γ.
Step 3: Deduce $B_L(\rho)$, $D_L(\rho)$ by using $P_1(\rho)$, $P_2(\rho)$, $Y_1(\rho)$, $Y_2(\rho)$ obtained in Step 2.

4. APPLICATION TO A SEMI-ACTIVE SUSPENSION SYSTEM

4.1 System definition and modeling

A dynamical model of the semi-active electro-rheological suspension system is illustrated in Figure 1 with further details available in Pham et al. (2021). The quarter-car model comprises the sprung mass m_s, with displacement $z_s(t)$, the unsprung mass m_{us}, with displacement $z_{us}(t)$, and the suspension components between them. The tire is modeled as a spring with stiffness k_t. The system dynamics near equilibrium are described by the following equations, based on Newton's second law.

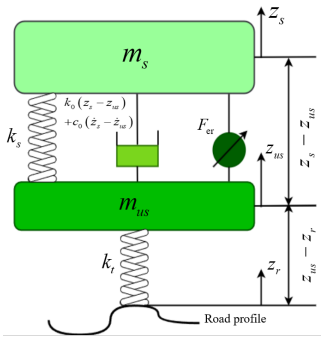

Fig. 1. 1/4 car model with semi-active suspension as presented in Pham et al. (2021)

$$\begin{cases} m_s \ddot{z}_s & = -F_s - F_d \\ m_{us} \ddot{z}_{us} & = F_s + F_d - F_t \end{cases} \qquad (23)$$

where $F_s = k_s(z_s - z_{us})$ is the spring force; $F_t = k_t(z_{us} - z_r)$ is the tire force; the damper force F_d is later given as in (24). z_s and z_{us} are the displacements of the sprung and unsprung masses, respectively; z_r is the road displacement input.
The damper model is chosen as:

$$\begin{cases} F_d & = k_0(z_s - z_{us}) + c_0(\dot{z}_s - \dot{z}_{us}) + F_{er} \\ \dot{F}_{er} & = -\frac{1}{\tau_s} F_{er} + \frac{f_c}{\tau_s} \cdot u \cdot tanh(k_1(z_s - z_{us}) \\ & \quad + c_1(\dot{z}_s - \dot{z}_{us})) \end{cases} \qquad (24)$$

where F_d is the total damper force; $c_0, c_1, k_0, k_1, f_c, \tau_s$ are constant parameters; z_s and z_{us} are the displacements of the sprung and unsprung masses, respectively. The control input u, which takes values in $[0, 1]$, is the voltage that provides the electrical field to control the ER damper.

4.2 LPV modelling

By selecting the system states as $x = [x_1, x_2, x_3, x_4, x_5]^T = [z_s - z_{us}, \dot{z}_s, z_{us} - z_r, \dot{z}_{us}, F_{er}]^T \in \mathbb{R}^5$, the measured variables $y = [\ddot{z}_s, \ddot{z}_{us}]^T \in \mathbb{R}^2$, choosing now the scheduling variable $\rho = tanh(k_1 x_1 + c_1(x_2 - x_4))$, the system dynamics can be written in the following LPV form:

$$\begin{cases} \dot{x} &= Ax + B(\rho)u + D_1\omega \\ y &= Cx + D_2\omega \end{cases} \tag{25}$$

where $n_x = 5$, $n_y = 2$ and $\omega = \begin{pmatrix} \omega_r \\ \omega_n \end{pmatrix}$, in which, $\omega_r = \dot{z}_r$ is the road profile derivative and ω_n is the sensor noises, and with

$$A = \begin{bmatrix} 0 & 1 & 0 & -1 & 0 \\ -\frac{(k_s+k_0)}{m_s} & -\frac{c_0}{m_s} & 0 & \frac{c_0}{m_s} & -\frac{1}{m_s} \\ 0 & 0 & 0 & 1 & 0 \\ \frac{(k_s+k_0)}{m_{us}} & \frac{c_0}{m_{us}} & -\frac{k_t}{m_{us}} & -\frac{c_0}{m_{us}} & \frac{1}{m_{us}} \\ 0 & 0 & 0 & 0 & -\frac{1}{\tau_s} \end{bmatrix},$$

$$C = \begin{bmatrix} -\frac{(k_s+k_0)}{m_s} & -\frac{c_0}{m_s} & 0 & \frac{c_0}{m_s} & -\frac{1}{m_s} \\ \frac{(k_s+k_0)}{m_{us}} & \frac{c_0}{m_{us}} & -\frac{k_t}{m_{us}} & -\frac{c_0}{m_{us}} & \frac{1}{m_{us}} \end{bmatrix},$$

$$B(\rho) = \begin{bmatrix} 0 \\ 0 \\ 0 \\ 0 \\ \frac{f_c}{\tau_s}\rho \end{bmatrix}, D_1 = \begin{bmatrix} 0 & 0 \\ 0 & 0 \\ -1 & 0 \\ 0 & 0 \\ 0 & 0 \end{bmatrix}, D_2 = \begin{bmatrix} 0 & 0.01 \\ 0 & 0.01 \end{bmatrix}.$$

4.3 Observer synthesis results

In this section, the proposed approach is applied and compared with the NLPV observer using gridding method presented in (Pham et al., 2021) (P observer) to highlight the advantages of a PID observer structure. As previously noted, the scheduling parameter $\rho = tanh(k_1 x_1 + c_1(x_2 - x_4))$ is constrained within the range $[-1, 1]$. In this work, the gridding method in (Wu, 1995) is applied to solve the LMI (11) in Theorem 1. We then choose a parameter dependent Lyapunov function and observer gains, as follows:

$$P_1(\rho) = P_{10} + \rho P_{11} \tag{26}$$

$$P_2(\rho) = P_{20} + \rho P_{21} \tag{27}$$

$$D_L(\rho) = D_{L0} + \rho D_{L1} \tag{28}$$

$$B_L(\rho) = B_{L0} + \rho B_{L1} \tag{29}$$

It is now explained how such matrices are obtained through the solution of Theorem 1. From (26) and (27),

$$\frac{\partial P_1}{\partial \rho} = P_{11}, \quad \frac{\partial P_2}{\partial \rho} = P_{21} \tag{30}$$

From (26) and (28), $Y_1(\rho) = -P_1(\rho)D_L(\rho)$ becomes

$$\begin{aligned} Y_1(\rho) &= -P_{10}D_{L0} - \rho(P_{10}D_{L1} + P_{11}D_{L0}) - \rho^2 P_{11}D_{L1} \\ &:= Y_{10} + \rho Y_{11} + \rho^2 Y_{12} \end{aligned} \tag{31}$$

where $Y_{10} = -P_{10}D_{L0}$; $Y_{11} = -P_{10}D_{L1} - P_{11}D_{L0}$; $Y_{12} = -P_{11}D_{L1}$.
From (27) and (29), $Y_2(\rho) = P_2(\rho)B_L(\rho)$ becomes

$$\begin{aligned} Y_2(\rho) &= P_{20}B_{L0} + \rho(P_{20}B_{L1} + P_{21}B_{L0}) + \rho^2 P_{21}B_{L1} \\ &= Y_{20} + \rho Y_{21} + \rho^2 Y_{22} \end{aligned} \tag{32}$$

where $Y_{20} = P_{20}B_{L0}$; $Y_{21} = P_{20}B_{L1} + P_{21}B_{L0}$; $Y_{22} = P_{21}B_{L1}$.
The LMI problem (11) considering $|\dot{\rho}| \leq \nu$ is solved for a set of N grid points as:

$$M(\rho_i) + B_n^T Z B_n < 0, i = 1, 2, ..., N \tag{33}$$

where $M(\rho_i) = \begin{bmatrix} M_{11}(\rho_i) & M_{12}(\rho_i) & M_{13}(\rho_i) \\ M_{12}(\rho_i)^T & M_{22}(\rho_i) & M_{23}(\rho_i) \\ M_{13}(\rho_i)^T & M_{23}(\rho_i)^T & -\gamma^2 I \end{bmatrix}$, with $M_{11}(\rho_i) = A(\rho_i)^T(P_{10} + \rho_i P_{11}) + C(\rho_i)^T(Y_{10} + \rho_i Y_{11} + \rho_i^2 Y_{12})^T + (P_{10} + \rho_i P_{11})A(\rho_i) + (Y_{10} + \rho_i Y_{11} + \rho_i^2 Y_{12})C(\rho_i) \pm \nu P_{11} + I$; $M_{12}(\rho_i) = C(\rho_i)^T(Y_{20} + \rho_i Y_{21} + \rho_i^2 Y_{22})^T - (P_{10} + \rho_i P_{11})C_L$; $M_{13}(\rho_i) = (P_{10} + \rho_i P_{11})D_1(\rho_i) + (Y_{10} + \rho_i Y_{11} + \rho_i^2 Y_{12})D_2(\rho_i)$; $M_{22}(\rho_i) = A_L^T(P_{20} + \rho_i P_{21}) + (P_{20} + \rho_i P_{21})A_L \pm \nu P_{21}$; $M_{23}(\rho_i) = (Y_{20} + \rho_i Y_{21} + \rho_i^2 Y_{22})D_2(\rho_i)$.
From solutions of (33), the matrices P_{10}, P_{11}, P_{20}, P_{21}, Y_{10}, Y_{11}, Y_{12}, Y_{20}, Y_{21}, Y_{22} are obtained.

$$\begin{bmatrix} -P_{10} & 0 \\ -P_{11} & -P_{10} \\ 0 & -P_{11} \end{bmatrix} \begin{bmatrix} D_{L0} \\ D_{L1} \end{bmatrix} = \begin{bmatrix} Y_{10} \\ Y_{11} \\ Y_{12} \end{bmatrix} \tag{34}$$

which leads to the observer matrices D_{L0} and D_{L1} as follows:

$$\begin{bmatrix} D_{L0} \\ D_{L1} \end{bmatrix} = \begin{bmatrix} -P_{10} & 0 \\ -P_{11} & -P_{10} \\ 0 & -P_{11} \end{bmatrix}^+ \begin{bmatrix} Y_{10} \\ Y_{11} \\ Y_{12} \end{bmatrix} \tag{35}$$

where $(\cdot)^+$ is the generalized inverse of matrix $(\cdot)$.

$$\begin{bmatrix} P_{20} & 0 \\ P_{21} & P_{20} \\ 0 & P_{21} \end{bmatrix} \begin{bmatrix} B_{L0} \\ B_{L1} \end{bmatrix} = \begin{bmatrix} Y_{20} \\ Y_{21} \\ Y_{22} \end{bmatrix} \tag{36}$$

which leads to the observer matrices B_{L0} and B_{L1} as follows:

$$\begin{bmatrix} B_{L0} \\ B_{L1} \end{bmatrix} = \begin{bmatrix} P_{20} & 0 \\ P_{21} & P_{20} \\ 0 & P_{21} \end{bmatrix}^+ \begin{bmatrix} Y_{20} \\ Y_{21} \\ Y_{22} \end{bmatrix} \tag{37}$$

where $(\cdot)^+$ is the generalized inverse of matrix $(\cdot)$.
The CVX toolbox (Grant and Boyd, 2014) and Sedumi solver (Sturm, 2001) are employed to solve the optimization problem presented in Theorem 1 at the gridded points which are defined by ρ as follows

$$\rho = [-1, -0.8, -0.6, -0.4, -0.2, 0, 0.2, 0.4, 0.6, 0.8, 1]$$

and the bounded value of $\dot{\rho}$ is $\nu_\rho = 1$.
Then, the varying observer gains $B_L(\rho)$ and $D_L(\rho)$ are calculated from the vertice observer gains as follows:

$$B_L(\rho) = B_{L0} + \rho B_{L1},\ D_L(\rho) = D_{L0} + \rho D_{L1}$$

4.4 Frequency domain analysis

Figures 2 and 3 present the Bode diagrams of the estimation error with respect to the road profile derivative and sensor noises for the proposed observers. Red line represent the Bode diagrams of the estimation error systems of the gridding PID observer and the gridding NLPV observer (green dot) at the frozen values of 11 grid points.

According to the plots, it can be concluded that the PID observer ensures a better disturbance and noise attenuation than the NLPV observer overall. The NLPV observer

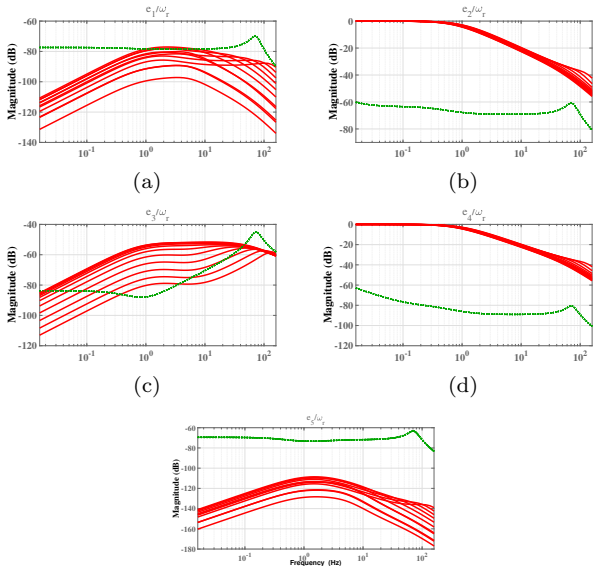

(a) (b) (c) (d) (e)

Fig. 2. Road effect performance : Bode magnitude of the transfer $\|e/\omega_r\|$: (a) $\|e_1/\omega_r\|$, (b) $\|e_2/\omega_r\|$, (c) $\|e_3/\omega_r\|$, (d) $\|e_4/\omega_r\|$ and (e) $\|e_5/\omega_r\|$.

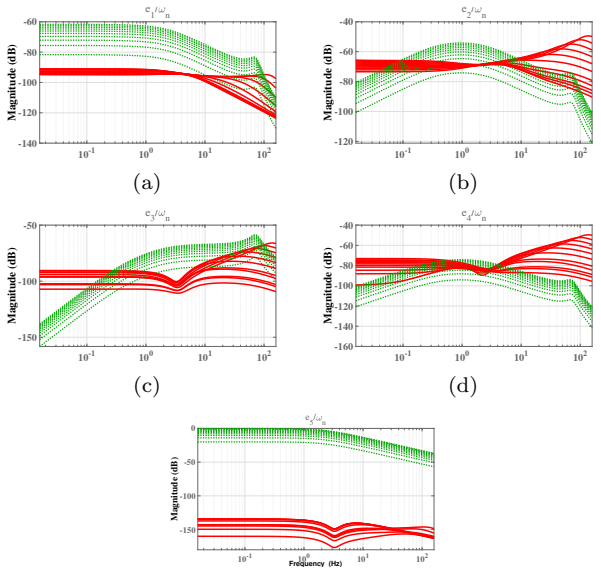

(a) (b) (c) (d) (e)

Fig. 3. Measurement noise sensitivity: Bode magnitude of the transfer $\|e/\omega_n\|$: (a) $\|e_1/\omega_n\|$, (b) $\|e_2/\omega_n\|$, (c) $\|e_3/\omega_n\|$, (d) $\|e_4/\omega_n\|$ and (e) $\|e_5/\omega_n\|$.

only achieves better noise attenuation results for two state estimation errors, e_2 and e_4 as seen in Fig 3(b-d), while the PID observer improves the rejection of the road profile derivative and measurement noise onto the fifth state estimation error e_5 (see Fig 2 (e)- Fig 3 (e)), which is related to the damping force F_{er}.

4.5 Time-domain simulation results

Two simulation scenarios are shown to evaluate the performance of the proposed observer. The initial state conditions for the quarter-car system (x_0), the gridding NLPV observer ($\hat{x}_{NLPV}(0)$), and the gridding PID observer ($\hat{x}_{PID}(0)$) are chosen as follows: $x_0 = [0,\ 0,\ 0,\ 0,\ 0]^T$ and $\hat{x}_{NLPV}(0) = \hat{x}_{PID}(0) = [0.015,\ -0.15,\ 0.0015,\ -0.15,\ 3]^T$
First simulation case:

- a sinusoidal signal.
- The control input u is constant at $u = 0.35$.

Figure 4 presents the simulation results, highlighting the performance of the gridding PID observer.
Second simulation case:

- The road profile input z_r follows ISO 8608 road profile signal (Type C) .
- The control input u is generated by a Skyhook controller.

The simulation results of the second test are presented in Figure 5. The stability of the PID observer within the closed-loop system is maintained even when the scheduling parameter varies rapidly.
To conclude both simulation results validate the effectiveness of the proposed observers design.

For quantitative comparison, the Normalized Root-Mean-Square Errors (NRMSE) and the Integral Time Absolute Error (ITAE) of the estimation errors are presented in Table 1. These results highlight the superior efficiency of the PID observer in the test cases.

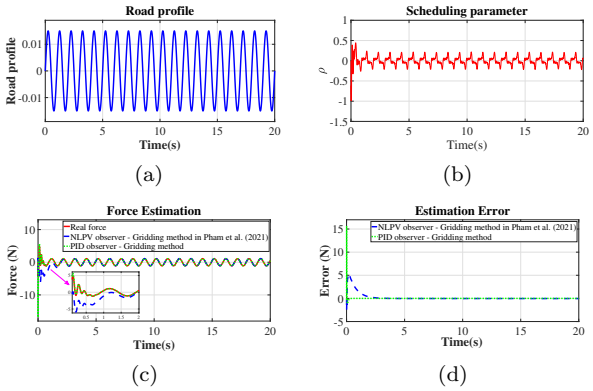

(a) (b) (c) (d)

Fig. 4. Simulation 1: (a) Road profile, (b) Scheduling parameter, (c) Damper force, (d) Estimation error.

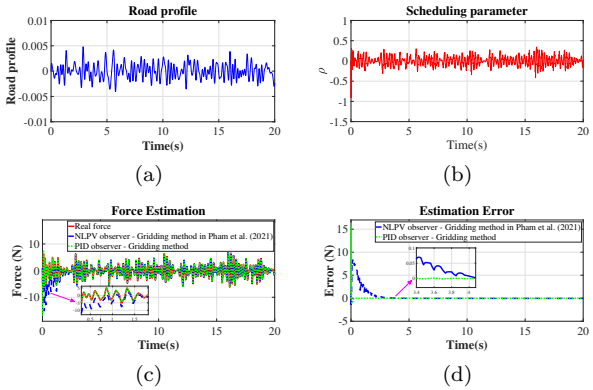

(a) (b) (c) (d)

Fig. 5. Simulation 2: (a) Road profile, (b) Scheduling parameter, (c) Damper force, (d) Estimation error.

Table 1. Normalized Root-Mean-Square Errors (NRMSE) and Integral Time Absolute Error (ITAE) of the simulation scenarios

Simulation scenario	NRMSE (%) for $[0-20s]$	
	NLPV observer	PID observer
Scenario 1	0.1099	0.0158
Scenario 2	0.0793	0.0154
Simulation scenario	NRMSE (%) for $[2-20s]$	
	NLPV observer	PID observer
Scenario 1	0.0204	2.1953×10^{-4}
Scenario 2	0.0095	4.6415×10^{-5}
Simulation scenario	ITAE for $[0-20s]$	
	NLPV observer	PID observer
Scenario 1	137.6	0.1083
Scenario 2	314.9	0.1155

5. CONCLUSION

In this paper, a proportional-integral-derivative observer has been proposed for linear parameter-varying systems, with a specific application to the estimation of the damper force in a semi-active suspension system. The nonlinear dynamics of the semi-active suspension are reformulated into an quasi-LPV model. By incorporating proportional, integral, and derivative actions, the PID observer improves performance and reduces the impact of unknown disturbances using an H_∞ performance criterion. The design methodology employs Finsler's Lemma to reformulate quadratic conditions into a linear matrix inequality optimization problem, ensuring both computational efficiency and stability. Simulations and frequency-domain analysis validate the effectiveness of the proposed method, emphasizing its potential for practical implementation in automotive suspension systems.

REFERENCES

Apkarian, P. and Noll, D. (2006). Nonsmooth h_∞ synthesis. *IEEE Transactions on Automatic Control*, 51(1), 71–86.

Csekő, L.H., Kvasnica, M., and Lantos, B. (2015). Explicit mpc-based rbf neural network controller design with discrete-time actual kalman filter for semiactive suspension. *IEEE Transactions on Control Systems Technology*, 23(5), 1736–1753.

Darouach, M., Boutat-Baddas, L., and Zerrougui, M. (2011). h_∞ observers design for a class of nonlinear singular systems. *Automatica*, 47(11), 2517–2525.

de Oliveira, M.S. and Pereira, R.L. (2021). On unknown input observers designs for discrete-time lpv systems with bounded rates of parameter variation. *European Journal of Control*, 58, 183–195.

Dugard, L., Sename, O., Aubouet, S., and Talon, B. (2012). Full vertical car observer design methodology for suspension control applications. *Control Engineering Practice*, 20(9), 832–845.

Gao, N., Darouach, M., Voos, H., and Alma, M. (2016). New unified h_∞ dynamic observer design for linear systems with unknown inputs. *Automatica*, 65, 43–52.

Grant, M. and Boyd, S. (2014). Cvx: Matlab software for disciplined convex programming, version 2.1.

Ichalal, D. and Mammar, S. (2015). On unknown input observers for lpv systems. *IEEE Transactions on Industrial Electronics*, 62(9), 5870–5880.

Iwasaki, T. and Shibata, G. (2002). Lpv system analysis via quadratic separator for uncertain implicit systems. *IEEE Transactions on Automatic Control*, 46(8), 1195–1208.

Koch, G., Kloiber, T., Pellegrini, E., and Lohmann, B. (2010). A nonlinear estimator concept for active vehicle suspension control. In *Proceedings of the 2010 American Control Conference*, 4576–4581. doi: 10.1109/ACC.2010.5530877.

Kulcsár, B., Bokor, J., and Shinar, J. (2010). Unknown input reconstruction for lpv systems. *International Journal of Robust and Nonlinear Control: IFAC-Affiliated Journal*, 20(5), 579–595.

Marx, B., Ichalal, D., Ragot, J., Maquin, D., and Mammar, S. (2019). Unknown input observer for lpv systems. *Automatica*, 100, 67–74.

Mohammadpour, J. and Scherer, C.W. (2012). *Control of linear parameter varying systems with applications*. Springer Science & Business Media.

Pérez-Estrada, A.J., Osorio-Gordillo, G.L., Darouach, M., Alma, M., and Olivares-Peregrino, V.H. (2018). Generalized dynamic observers for quasi-lpv systems with unmeasurable scheduling functions. *International Journal of Robust and Nonlinear Control*, 28(17), 5262–5278.

Pham, T.P., Sename, O., and Dugard, L. (2019). Unified hinf observer for a class of nonlinear lipschitz systems: application to a real er automotive suspension. *IEEE Control Systems Letters*.

Pham, T.P., Sename, O., and Dugard, L. (2021). A nonlinear parameter varying observer for real-time damper force estimation of an automotive electro-rheological suspension system. *International Journal of Robust and Nonlinear Control*, 31(17), 8183–8205.

Savaresi, D., Favalli, F., Formentin, S., and Savaresi, S. (2019). On-line damping estimation in road vehicle semi-active suspension systems. *IFAC-PapersOnLine*, 52(5), 679–684.

Savaresi, S.M., Poussot-Vassal, C., Spelta, C., Sename, O., and Dugard, L. (2010). *Semi-active suspension control design for vehicles*. Elsevier.

Sename, O. (2025). *Linear Parameter-Varying Control: Theory and Application to Automotive Systems*. John Wiley & Sons, Inc., Hoboken, New Jersey.

Sename, O., Gaspar, P., and Bokor, J. (2013). *Robust control and linear parameter varying approaches: application to vehicle dynamics*, volume 437. Springer.

Sturm, J. (2001). Sedumi 1.05.

Tseng, H.E. and Hrovat, D. (2015). State of the art survey: active and semi-active suspension control. *Vehicle system dynamics*, 53(7), 1034–1062.

Tudón-Martínez, J.C., Fergani, S., Sename, O., Martinez, J.J., Morales-Menendez, R., and Dugard, L. (2015). Adaptive road profile estimation in semiactive car suspensions. *IEEE Transactions on Control Systems Technology*, 23(6), 2293–2305.

Wu, F. (1995). *Control of Linear Parameter Varying Systems*. Ph.D. thesis, University of California, Berkeley.

Yi, K. and Suk Song, B. (1999). Observer design for semiactive suspension control. *Vehicle System Dynamics*, 32(2-3), 129–148.